AMSR-E/Aqua Daily L3 12.5 km Brightness Temperature, Sea Ice Concentration, & Snow Depth Polar Grids, Version 3

USER GUIDE

How to Cite These Data

As a condition of using these data, you must include a citation:

Cavalieri, D. J., T. Markus, and J. C. Comiso. 2014. *AMSR-E/Aqua Daily L3 12.5 km Brightness Temperature, Sea Ice Concentration, & Snow Depth Polar Grids, Version 3*. [Indicate subset used]. Boulder, Colorado USA. NASA National Snow and Ice Data Center Distributed Active Archive Center. https://doi.org//10.5067/AMSR-E/AE_SI12.003. [Date Accessed].

FOR QUESTIONS ABOUT THESE DATA, CONTACT NSIDC@NSIDC.ORG

FOR CURRENT INFORMATION, VISIT https://nsidc.org/data/AE_SI12

National Snow and Ice Data Center

TABLE OF CONTENTS

1 DATA DESCRIPTION

This Level-3 gridded product (AE_SI12) includes brightness temperatures at 18.7 through 89.0 GHz, sea ice concentration, and snow depth over sea ice.

1.1 Format

Data are stored in Hierarchical Data Format - Earth Observing System (HDF-EOS) format.

1.2 Data Fields

Refer to Appendix A – Level-3 12.5 km Sea Ice Data Fields for a list of HDF-EOS data fields.

1.3 File Naming Convention

This section explains the file naming convention used for this product with examples.

Example file name:

```
AMSR_E_L3_SeaIce12km_V15_20080207.hdf
AMSR_E_L3_SeaIce12km_X##_yyyymmdd.hdf
```

Refer to Table 1 for the values of the file name variables listed above.

Table 1. Variable Values for the File Name

Variable	Description
X	Product Maturity Code (Refer to Table 2 for valid values.)
##	file version number
yyyy	four-digit year
mm	two-digit month
dd	two-digit day
hdf	Hierarchical Data Format (HDF)

Table 2. Variable Values for the Product Maturity Code

Variables	Description
P	Preliminary - refers to non-standard, near-real-time data available from NSIDC. These data are only available for a limited time until the corresponding standard product is ingested at NSIDC.
B	Beta - indicates a developing algorithm with updates anticipated.

Variables	Description
T	Transitional - period between beta and validated where the product is past the beta stage, but not quite ready for validation. This is where the algorithm matures and stabilizes.
V	Validated - products are upgraded to Validated once the algorithm is verified by the algorithm team and validated by the validation teams. Validated products have an associated validation stage. Refer to Table 3 for a description of the stages.

Table 3. Validation Stages

Validation Stage	Description
Stage 1	Product accuracy is estimated using a small number of independent measurements obtained from selected locations, time periods, and ground-truth/field program efforts.
Stage 2	Product accuracy is assessed over a widely distributed set of locations and time periods via several ground-truth and validation efforts.
Stage 3	Product accuracy is assessed, and the uncertainties in the product are well-established via independent measurements made in a systematic and statistically robust way that represents global conditions.

Table 4 provides examples of file name extensions for related files that further describe or supplement data files.

Table 4. Related File Extensions and Descriptions

Extensions for Related Files	Description
.jpg	Browse data
.qa	Quality assurance information
.ph	Product history data
.xml	Metadata files

1.4 File Size

Each daily granule is approximately 53 MB.

1.5 Spatial Coverage

1.5.1 Spatial Coverage Map

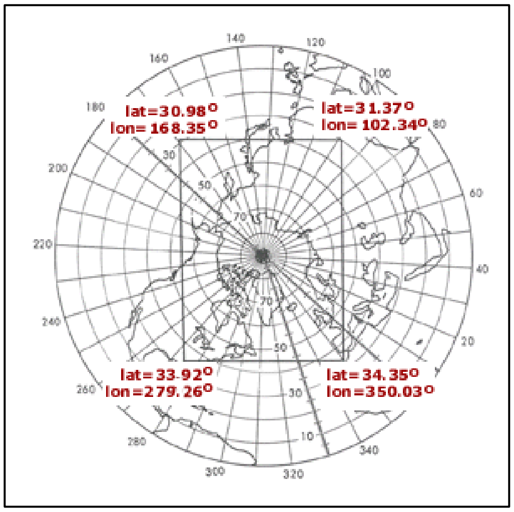

Figure 1. Northern Hemisphere

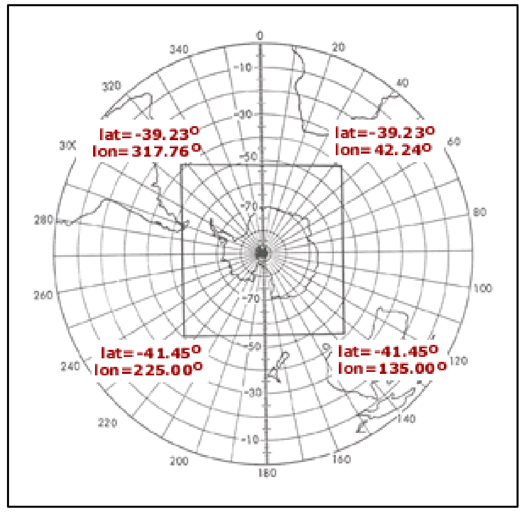

Figure 2. Southern Hemisphere

1.5.2 Spatial Resolution

The spatial resolution of the polar grids is 12.5 km.

1.5.3 Projection and Grid Description

1.5.3.1 Projection

Brightness temperature grids are in a polar stereographic projection, which specifies a projection plane such as the grid, tangent to the Earth at 70 degrees. The planar grid is designed so that the grid cells at 70 degrees latitude are 12.5 km by 12.5 km. For more information on this topic please refer to Pearson (1990) and Snyder (1987).

The polar stereographic projection often assumes that the plane (grid) is tangent to the Earth at the pole. Thus, there is a one-to-one mapping between the Earth's surface and grid with no distortion at the pole. Distortion in the grid increases as the latitude decreases because more of the Earth's surface falls into any given grid cell. At the edge of the northern polar grid distortion reaches 31 percent. The southern polar grid has a maximum distortion of 22 percent. To minimize the distortion, the projection is true at 70 degrees rather than at the poles. This increases the distortion at the poles by three percent and decreases the distortion at the grid boundaries by the same amount. The latitude of 70 degrees was selected so that little or no distortion would occur in the marginal ice zone. Another result of this assumption is that fewer grid cells will be required as the Earth's surface is more accurately represented.

The polar stereographic formulae for converting between latitude/longitude and X-Y grid coordinates are taken from (Snyder 1982). This projection assumes a Hughes ellipsoid with a radius of 3443.992 nautical mi or 6378.273 km and an eccentricity (e) of 0.081816153 (or e^2 = 0.006693883). The structural metadata (StructMetadata.0) built into the HDF-EOS data file lists the squared eccentricity value rounded to four significant digits (0.006694).

1.5.3.2 Grid Description

Northern Hemisphere: 608 columns by 896 rows
Southern Hemisphere: 632 columns by 664 rows

The origin of each x, y grid is the pole. The grids' approximate outer boundaries are defined in the following table. Corner points are listed; apply values to the polar grids reading clockwise from upper left. Interim rows define boundary midpoints.

Table 5. North Polar

X (km)	Y (km)	Latitude (deg)	Longitude (deg)	Pixel Location
-3850	5850	30.98	168.35	corner
0	5850	39.43	135.00	midpoint
3750	5850	31.37	102.34	corner
3750	0	56.35	45.00	midpoint
3750	-5350	34.35	350.03	corner
0	-5350	43.28	315.00	midpoint
-3850	-5350	33.92	279.26	corner
-3850	0	55.50	225.00	midpoint

Table 6. South Polar

X (km)	Y (km)	Latitude (deg)	Longitude (deg)	Pixel Location
-3950	4350	-39.23	317.76	corner
0	4350	-51.32	0.00	midpoint
3950	4350	-39.23	42.24	corner
3950	0	-54.66	90.00	midpoint
3950	-3950	-41.45	135.00	corner
0	-3950	-54.66	180.00	midpoint
-3950	-3950	-41.45	225.00	corner
-3950	0	-54.66	270.00	midpoint

For this product, there are files that contain geolocation and pixel-area tools, which provide the same functionality for all polar stereographic passive microwave sea ice data sets at NSIDC. These tools include a FORTRAN routine called locate.for, a latitude/longitude grid, and a pixel-area grid.

The following geocoordinate FORTRAN tools are available via FTP:

- **locate.for**: A FORTRAN routine that allows the user to enter an i,j coordinate and get the corresponding latitude/longitude coordinate, and vice versa.
- **mapll.for** and **mapxy.for**: Subroutines that are associated with the locate.for program. These programs need to be compiled, but are not run explicitly. They are called by locate.for. Thus, the user should compile these programs with locate.for and then use locate to do the conversions.

The latitude/longitude grids are in binary format and are stored as long word integers (4 byte) scaled by 100,000. Each array location (i,j) contains the latitude or longitude value at the center of the corresponding data grid cells. These files are available via FTP.

Table 7. File Variables

Variables	Description
pss	polar stereographic southern projection
psn	polar stereographic northern projection
06, 12, & 25	6 km, 12 km, and 25 km, respectively
lat	latitude grid
lon	longitude grid
area	pixel area

1.6 Temporal Coverage

Data were collected from 01 June 2002 to 4 October 2011.

1.6.1 Temporal Resolution

Brightness temperatures and sea ice concentrations are daily averages, daily ascending averages, and daily descending averages. Snow depths are five-day running averages.

1.7 Parameter or Variable

Brightness Temperature (K)
Snow Depth on Sea Ice
Sea Ice Concentration
Sea Ice Concentration differences between Bootstrap Basic Algorithm (BBA) and Enhanced NASA Team (NT2)

Refer to Appendix A – Level-3 12.5 km Sea Ice Data Fields for more information regarding the Sea Ice parameters.

1.7.1 Parameter Description

This data set contains the following gridded parameters:

- Vertical and horizontal brightness temperatures for the following channels. Separate HDF-EOS fields are provided for ascending, descending, and daily averages.
  - 18.7 GHz
  - 23.8 GHz
  - 36.5 GHz
  - 89.0 GHz
- Arctic sea ice concentration using the NT2 algorithm. Separate HDF-EOS fields are provided for ascending, descending, and daily averages.
- Antarctic sea ice concentration using the NT2 algorithm. Separate HDF-EOS fields are provided for ascending, descending, and daily averages.
- Arctic and Antarctic sea ice concentration differences between BBA and NT2. Separate HDF-EOS fields are provided for ascending, descending, and daily averages.
- Arctic and Antarctic five-day snow depth over sea ice, excluding Arctic perennial ice regions.

2 SOFTWARE AND TOOLS

For tools that work with AMSR-E data, see the Tools for AMSR-E Data Web page.

For general tools that work with HDF-EOS data, see the NSIDC HDF-EOS Web page.

3 DATA ACQUISITION AND PROCESSING

3.1 Theory of Measurements

Sea ice concentration products are used to understand the spatial characterization of sea ice cover and to calculate sea ice extent and area for time series analyses and process studies in the Arctic and Antarctic. Passive microwave data are particularly useful for sea ice studies because of the relatively high contrast in emissivities between open water and sea ice. This contrast is frequency-dependent; contrast increases with decreasing channel frequency. In most algorithms, atmospheric effects are assumed constant. The satellite-received radiation, expressed as a Brightness Temperature (T_b), is as follows (Cavalieri and Comiso 2000):

$T_b = T_{bw}C_w + T_{bi}C_i$ **(Equation 1)**

Where:

T_{bw} = brightness temperature of open water
T_{bi} = brightness temperature of sea ice
C_w = fraction of open water within instrument field-of-view
C_i = fraction of sea ice concentration within the instrument field-of-view

Sea ice concentration (C_I), corresponding to an observed T_b over a sea-ice-covered region (T_b), is derived as follows:

$$C_i = \frac{T_b - T_{bw}}{T_{bi} + T_{bw}}$$ **(Equation 2)**

The AMSR-E sea ice algorithms use this equation, but the channels and methods to derive sea ice concentrations are different. Values of brightness temperature of open water, brightness temperature of sea ice, and brightness temperature all include contributions from the intervening atmosphere. Brightness temperature of sea ice varies spatially because of spatial changes in emissivity and temperature of ice, while brightness temperature of open water is constant for open water within the ice pack.

3.2 Data Source

Observations for the 18.7, 23.8, 36.5, and 89 GHz channels, at native resolutions, from the AMSR-E/Aqua L2A Global Swath Spatially-Resampled Brightness Temperatures are gridded into 12.5 km grid cells using a drop-in-the-bucket method where the grid cell that contains the center of the observation footprint is given the whole weight of the observation. With this procedure, the number of observations is always in whole numbers. All valid brightness temperature observations within the extent of the polar grids are binned into grid cells, including land observations.

3.3 Derivation Techniques and Algorithms

Depending on the parameter being investigated, such as sea ice concentration or snow depth on sea ice, a different algorithm is used. Each algorithm is discussed in the following paragraphs.

3.3.1 Sea Ice Concentration

The 12.5 km sea ice concentration product is generated using the Enhanced NASA Team (NT2) algorithm described by Markus and Cavalieri (2000) for both the Arctic and the Antarctic. NT2 sea ice concentrations are calculated using the individual Level 2-A swaths rather than using gridded averaged brightness temperatures in order to make the atmospheric corrections on an orbit-by-orbit basis before obtaining daily average ice concentrations. However, previous AE_SI12 versions employed the Bootstrap Basic Algorithm (BBA) described by Comiso (1995) for the Antarctic. Now the BBA is only used in the sea ice concentration difference between the BBA and the NT2 (BBA-NT2) for both hemispheres.

The original NASA Team algorithm is based on techniques described in Cavalieri et al. (1984) and Gloersen and Cavalieri (1986). The NT2 algorithm (Markus and Cavalieri 2000) identifies two ice types for both the Arctic and the Antarctic:

Table 8. Polar Ice Types

Arctic	**Antarctic**
first-year ice	Type A ice consists primarily of first year ice
multiyear ice	Type B represents sea ice with a heavy snow cover resulting in increased scattering at 37V.

In this algorithm, the primary source of error is attributed to conditions in the surface layer such as surface glaze and layering (Comiso et al. 1997), which can significantly affect the horizontally polarized 18.7 GHz brightness temperature (Matzler et al. 1984) leading to increased PR(18) values and thus an underestimation of sea ice concentration. The use of the horizontally polarized channels makes it imperative to resolve a third ice type to overcome the difficulty of surface effects on the emissivity of the horizontally polarized component.

Thus, one advantage of using the NT2 algorithm is that it uses the 89 GHz channels because the horizontally polarized 89 GHz data are less affected by surface conditions than the horizontally polarized 18.7 GHz data (Matzler et al. 1984), and the 89 GHz channels have successfully been used in sea ice concentration retrievals under clear atmospheric conditions. As a result, this algorithm can identify more complex ice types resulting from surface glaze and layering in the snow cover. The thin-ice bias is reduced through the use of the third ice type. The third ice type consists of surface glaze and layering of sea ice with snow cover. This type of ice primarily occurs in the Antarctic.

The Spectral Gradient Ratios (GR) and Polarization Ratios (PRs) are calculated from the observed and modeled brightness temperatures using the following two equations:

The Polarization Equation:

$$PR(\nu) = \frac{T_B(\nu,V) - T_B(\nu,H)}{T_B(\nu,V) + T_B(\nu,H)} \quad \textbf{(Equation 3)}$$

The Spectral Gradient Ratio Equation:

$$GR(\nu_1, \nu_2, p) = \frac{T_B(\nu_1,p) - T_B(\nu_2,p)}{T_B(\nu_1,p) + T_B(\nu_2,p)}$$ **(Equation 4)**

Where:
T_b is the brightness temperature at frequency *v* for the polarized component *p* (vertical (V) or horizontal (H)).

The actual radiance ratios used in the NT2 algorithm are $PR_R(18)$, $PR_R(89)$, GR (89, 18, H-pol), and GR (89, 18, V-pol) where the subscript R refers to a rotation of axes. This rotation is done in the NT PR(18)-GR(37, 18, V-pol) domain, with the axes rotated through an angle, φ, until the ice-type lines (the FY-MY line for the Arctic and the A–B line for the Antarctic) are parallel to the GR axis. The rotated PR is defined by:

$$PR(18) = -GR(37V18V)\sin\phi + PR(18)\cos\phi$$ **(Equation 5)**

and is independent of the two ice types. Next, we make use of the difference between two gradient ratios

$$\Delta GR = GR\big(89{,}18, H_{-pol}\big) - \mathrm{GR}(89{,}18, V_{-pol})$$ **(Equation 6)**

to resolve the ambiguity between pixels with true low sea ice concentration and pixels with significant scattering (defined as Ice Type C). Therefore, ΔGR serves as an indicator of the presence of Ice Type C. The higher the value of ΔGR the higher the amount of layering within a pixel. The retrieval of Ice Type C is applied to both, the Arctic and the Antarctic, oceans. Finally, a third parameter is defined to avoid the ambiguity between changes in sea ice concentration and changes in atmospheric conditions, because of the higher sensitivity of the 89-GHz channels to atmospheric variability compared to the lower frequency channels. This third parameter is the rotated PR(89), $PR_R(89)$, computed from the PR(89)-GR(37V18V) domain analogous to the calculation of $PR_R(18)$ but with a different angle.

The algorithm quantifies atmospheric effects by calculating brightness temperatures for each channel using a forward atmospheric radiative transfer model (Kummerow 1993) that incorporates four surface types: first-year ice, multiyear ice, Type C, and open water. Beginning with version 3, the Southern Hemisphere sea ice concentration algorithm no longer uses the Level-2A land flag and only uses the updated land mask for surface type classification. Thus, the 89 GHz channels together with a forward radiative transfer model provide ice concentrations under all atmospheric conditions. Figure 3 shows the general flow of the algorithm. First brightness temperatures are calculated for the four surface types and all weather conditions, currently 12. The response of the brightness temperatures to different weather conditions is calculated using the atmospheric radiative transfer model. The input data for the model consists of several things such as: the emissivities of the different surface types taken from Table 4-1 in Eppler et al. (1992) with modifications to achieve agreement between modeled and observed ratios, different cloud properties, specifically cloud base, cloud top, and cloud liquid water, taken from Fraser et al. (1975), and average atmospheric temperature and humidity profiles for summer and winter conditions taken from Antarctic research stations. Brightness temperatures are calculated for all possible ice concentration combinations in one percent increments, and the following ratios were calculate for each increment: $PR_R(18)$, $PR_R(89)$, and ΔGR. This creates a prism in which each element within this space contains a vector with the three ratios: $PR_R(18)$, $PR_R(89)$, and ΔGR. The subscript R refers to a rotation of axes in PR-GR space by the angle so that $PR_R(18)$ and $PR_R(89)$ are independent of ice types A and B in the Antarctic, and first-year and multiyear ice for the Arctic. For each pixel, the observed brightness temperatures are used to create a vector with the same ratios. The ice concentration for a pixel is determined where the difference between an observed and a modeled ratio is smallest.

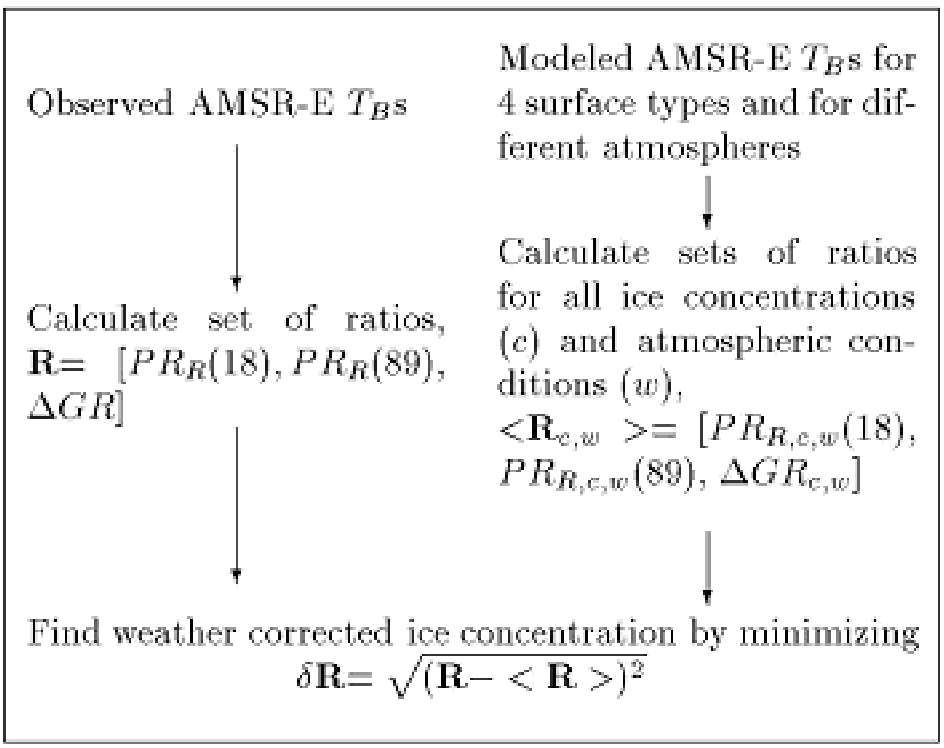

Figure 3. Flow Diagram of Enhanced NASA Team Algorithm

While for the Antarctic the algorithm resolves fractions between Ice Types A, B, and C, and open water, in the Arctic we also resolve a thin ice type. Using a GR(37V19V) threshold of -0.02, we either resolve Ice Type C for pixels where GR(37V19V) is below this threshold, or thin ice for pixels where GR(37V19V) is above this threshold. A limitation, of course, is that mixtures of thin ice and thicker ice with layering cannot be resolved.

The algorithm eliminates spurious sea ice concentrations over open ocean by employing weather filters previously used for SSM/I (Gloersen and Cavalieri 1986; Cavalieri et al. 1995). Ice concentrations for image pixels with GR(37V19V) values greater than 0.05 and GR(2219) values greater than 0.045 are set to zero.

Although a land mask is applied to the ice concentration maps, land spillover still leads to erroneous ice concentrations along the coast lines adjacent to open water. This makes operational usage of these maps cumbersome. Therefore, a land spillover correction scheme is applied on the maps.

3.3.2 Sea Ice Concentration Difference

The BBA (Comiso 1995) is used in the calculation of sea ice concentration differences between the BBA and the NT2 (BBA-NT2) for both hemispheres. Comiso calculated tie points for consolidated ice (T_{bi}) and open water (T_{bw}) with two sets of channels: 18.7V GHz and 37V GHz (called V1937), and 37H GHz and 37V GHz (HV37). Using these channels for the retrieval of sea ice concentration ensures consistency with historical sea ice products, beginning with SMMR.

3.3.3 Snow Depth on Sea Ice

Snow depth over sea ice is reported as a 5-day running average, which is based on the current day and the previous four days. The 12.5 km snow depth on sea ice product is generated using the AMSR-E snow-depth-on-sea-ice algorithm described by Markus and Cavalieri (1998) for both the Arctic and the Antarctic. However, this algorithm is only valid over seasonal ice. The snow depth on sea ice is calculated using the spectral gradient ratio of the 18.7 GHz and 36.5 GHz vertical polarization channels:

$$h_s = a_1 + a_2 GRV(ice) \quad \textbf{(Equation 7)}$$

Where:

Table 9. Equation 7 Variables

Variable	Description
h_s	Snow depth in meters
a_1	2.9[1]
a_2	-782[1]
GRV(ice)	Spectral gradient ratio corrected for the sea ice concentration
[1]Coefficients derived from the linear regression of in situ snow depth measurements on microwave data.	

$$GRV(ice) = \frac{T_b(37V) - T_b(18V) - k_1(1-C)}{T_b(37V) + T_b(18V) - k_2(1-C)}$$ **(Equation 8)**

Where:

Table 10. Equation 8 Variables

Variable	Description
k_1	$T_{bo}(37V)$-$T_{bo}(18V)$
k_2	$T_{bo}(37V)$+$T_{bo}(18V)$
T_{bo}	The Open Water Brightness Temperatures (T_{bo}) are average values from open ocean areas and are used as constants.
C	Sea Ice Concentration

The principal idea of the algorithm is similar to the AMSR-E snow-on-land algorithm (Kelly et al. 2003) utilizing the assumptions that scattering increases with increasing snow depth and that the scattering efficiency is greater at 36.5 GHz than at 18.7 GHz. For snow-free sea ice, the gradient ratio is close to zero and it becomes more and more negative as the snow depth and grain size increases. The correlation of regional in situ snow depth distributions and satellite-derived snow depth distributions is 0.81. The upper limit for snow depth retrievals is 50 cm, which is a result of the limited penetration depth at 18.7 and 36.5 GHz.

The algorithm is applicable to dry snow conditions only. At the onset of melt, the emissivity of both the 18.7 GHz and the 36.5 GHz channels approach unity (that of a blackbody) and the gradient ratio approaches zero initially before becoming positive. Thus, snow depth is indeterminate under wet snow conditions. Snow, which is wet during the day, frequently refreezes during the night. This refreezing results in very large grain sizes (Colbeck 1982), which leads to a reduced emissivity at 36.5 GHz relative to 18.7 GHz, thereby decreasing GRV(ice) and thus leads to an overestimate of snow depth. These thaw-freeze events cause large temporal variations in the snow depth retrievals. This temporal information is used in the algorithm to flag the snow depths as unretrievable from those periods with large fluctuations.

As in situ grain size measurements are even less frequently collected than snow depth measurements, the influence of grain size variations could not be incorporated into the algorithm. Because of the uncertainties in grain size and density variations as well as sporadic weather effects, AMSR-E daily snow depth products are five-day running averages similar to the AMSR-E snow depth on land product.

Figure 4 summarizes the snow depth algorithm. Snow depths are retrieved for the entire Southern Ocean, but only for the seasonal sea ice zones in the Arctic because the retrieval of Arctic snow depth is complicated by the presence of multiyear ice, which has a signature similar to snow cover on first-year ice. Both multiyear ice and deep snow on top of first-year ice results in increasingly negative values for the spectral GR; therefore, the algorithm only retrieves snow depth in the seasonal sea ice zones and in regions where the value of GR(37V19V) is greater than -0.02. This threshold corresponds to multiyear ice concentration of less than 20 percent. Where GR(37V19V) is less than -0.02, the algorithm flags pixels as multiyear ice. Because of the higher sensitivity of snow depth retrievals to ice concentration less than 20 percent, the algorithm limits snow depth retrievals to ice concentration between 20 -100 percent. Ice concentrations less than 20 percent appear almost exclusively near the ice edge.

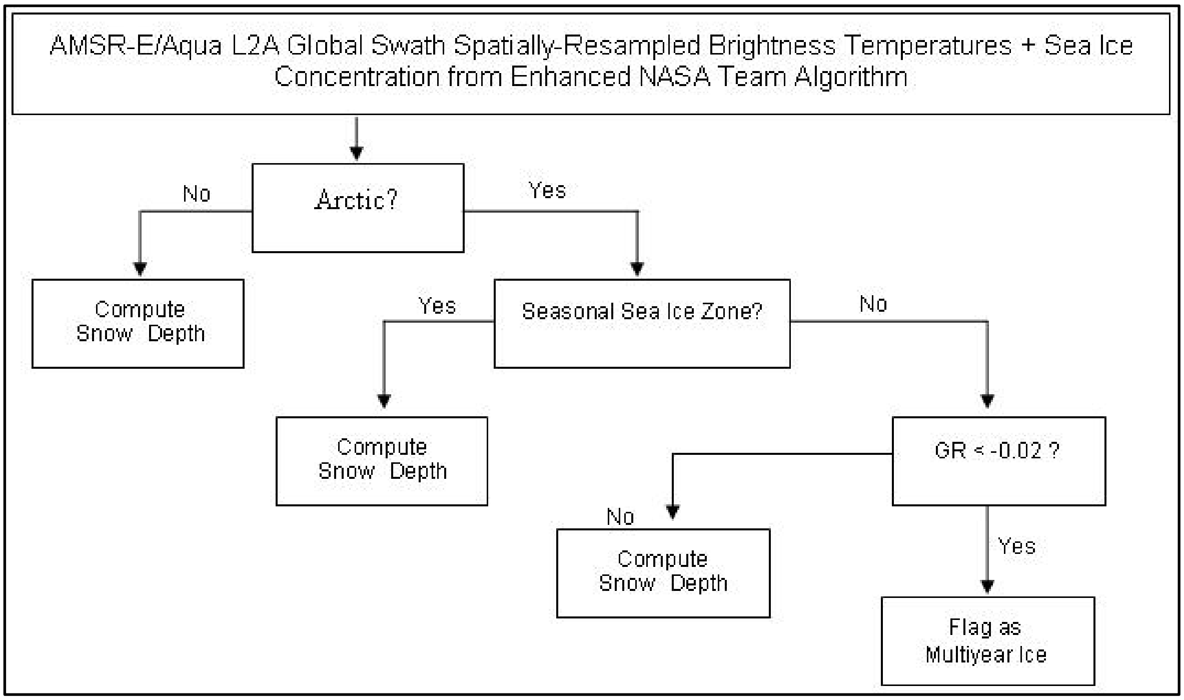

Figure 4. Processing Sequence for AMSR-E 25 km Sea Ice Products

3.3.4 Processing Steps

Figure 5 summarizes the input products and algorithms used to create gridded AMSR-E 12.5 km sea ice products.

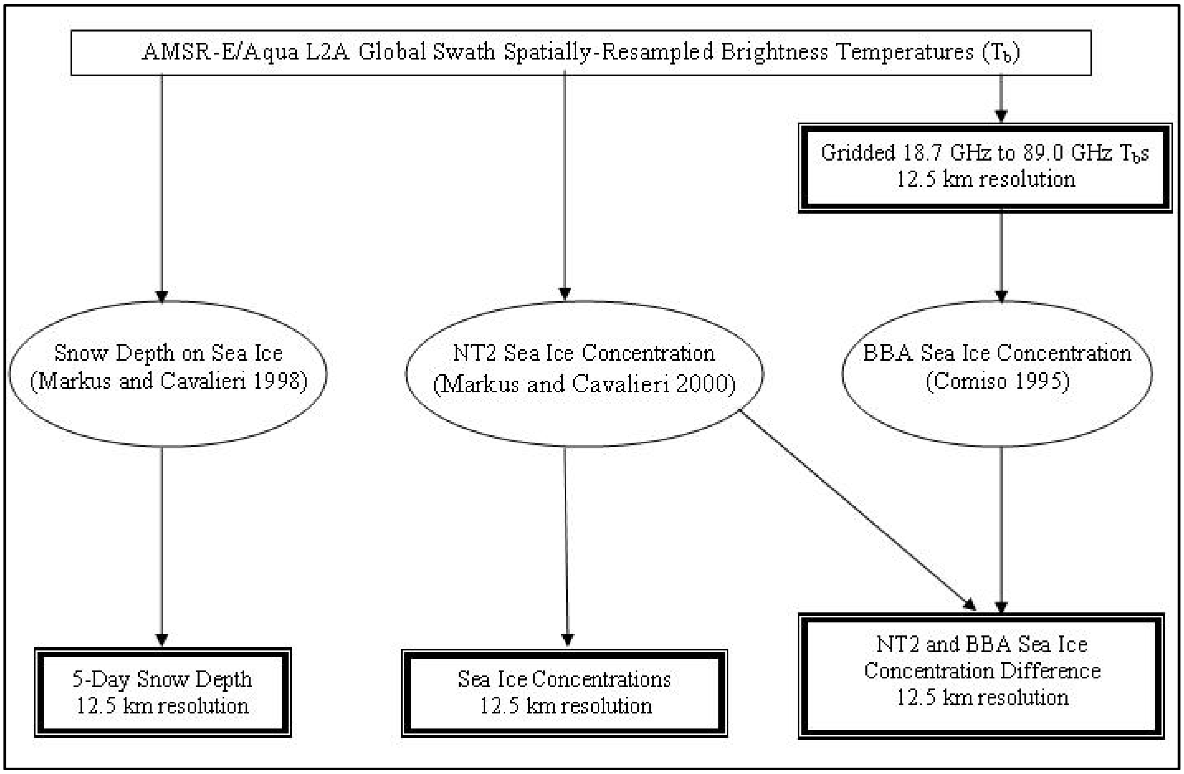

Figure 5. Processing Sequence for AMSR-E 12.5 km Sea Ice Products

The AMSR-E/Aqua L2A Global Swath Spatially-Resampled Brightness Temperatures are binned into 12.5 km grid cells using a drop-in-the-bucket method where the grid cell that contains the center of the observation footprint is given the whole weight of the observation. With this procedure, the number of observations is always in whole numbers. All valid brightness temperature observations within the extent of the polar grids are binned into grid cells, including land observations.

After input Level-2A brightness temperatures are binned into 12.5 km grid cells, the ascending, descending, and daily data are averaged. The daily average is not simply an average of ascending and descending orbits because a given pixel could have, for example, three measurements from ascending orbits and two from descending orbits. Instead, the daily average is of all the observations for that grid cell. For example, if A = ascending and B = descending:

$$\frac{\frac{A1+A2}{2}+\frac{B1+B2+B3}{3}}{2}$$ **(Equation 9)**

is not equal to:

$$\frac{A1+A2+B1+B2+B3}{5}$$ **(Equation 10)**

However, this biases day-time ascending orbits over night-time descending.

3.3.4.1 Sea Ice and Snow Melt Masks

Beginning with algorithm version V12, the sea ice and snow melt masks used for the Northern Hemisphere snow depth on sea ice parameter are stored within this data set. The masks from the most recent HDF file are used to generate each new HDF file. If the masks used are more than seven days old, the metadata science quality flag is set to *Suspect*.

The multiyear mask field in the HDF file refers to the multiyear sea ice mask. A default mask is used to initialize the multiyear mask on the first day of mission and also to reset the mask on the first processing date in October of each year.

The variability 5-day field in the HDF file refers to the snow melt mask. The snow melt mask corresponds to the running 5-day snow melt product, and its date must match that of the multiyear mask. The snow melt mask is reset at the same time as the multiyear mask.

3.3.4.2 Land Masks

The AMSR-E sea ice product utilizes a 12.5 km Northern Hemisphere land mask (amsr_gsfc_12n.hdf) and a 12.5 km Southern Hemisphere land mask (amsr_nic_12s.hdf). The North land mask is identical to gsfc_12n.msk and was last updated in 1997. See NSIDC's Polar Stereo web page for more details. The South land mask includes an updated ice shelf definition created by the National Ice Center Science Department in June 2011 and an updated shoreline developed from ENVISAT and RADARSAT imagery from October 2009 to April 2010.

A 1-byte integer array is included in each HDF file.

amsr_gsfc_12n.hdf: 608 columns x 896 rows
Values are 0 (water) and 1 (land).
amsr_nic_12s.hdf: 632 columns x 664 rows
Values are 0 (water), 1 (land), and 2 (coast).

3.3.5 Version History

Changes to the Version 3 (V15-stage1) algorithm for these data include:

- Use of the most recent version (Version 3) of the AMSR-E/Aqua L2A Global Swath Spatially-Resampled Brightness Temperatures data as input
- An improved Antarctic land mask
- No longer uses the Level-2A land flag and only uses the updated land mask for surface type classification in the Southern Hemisphere sea ice concentration algorithm

- Inclusion of ISO lineage metadata

Refer to the AMSR-E Data Versions Web page for a summary of changes since the start of mission

3.4 Error Sources

Ashcroft and Wentz (2000) discuss errors in the source Level-2A brightness temperatures that were binned into 12.5 km grid cells for this sea ice product. In the sea ice concentration algorithm, the primary source of error is attributed to conditions in the surface layer such as surface glaze and layering (Comiso et al. 1997), which can significantly affect the horizontally polarized 18.7 GHz brightness temperature (Matzler et al. 1984) leading to increased PR(18) values and thus underestimates in ice concentration.

Sources of error in the retrieval of snow depth on sea ice also include inherent errors in sea ice concentration, uncertainty in the linear relationship between snow depth and the AMSR-E brightness temperatures, undetected snow wetness, snow grain size and snow density variability, and sensitivity to extreme weather effects.

3.5 Quality Assessment

Each HDF-EOS file contains core metadata with Quality Assessment (QA) metadata flags that are set by the Science Investigator-led Processing System (SIPS) at the Global Hydrology and Climate Center (GHCC) prior to delivery to NSIDC. A separate metadata file in XML format is also delivered to NSIDC with the HDF-EOS file; it contains the same information as the core metadata. Three levels of QA are conducted with the AMSR-E Level-2 and -3 products: automatic, operational, and science QA. If a product does not fail QA, it is ready to be used for higher-level processing, browse generation, active science QA, archive, and distribution. If a granule fails QA, SIPS does not send the granule to NSIDC until it is reprocessed. Level-3 products that fail QA are never delivered to NSIDC (Conway 2002).

3.5.1 Automatic QA

Weather filters are employed for the Level-3 sea ice products to eliminate spurious sea ice concentrations over open ocean resulting from varying atmospheric emission. The weather filters are based on threshold values for the spectral gradient radio and thresholds derived from brightness temperature differences. Sea ice products are checked to see if ice concentration values fall within reasonable limits. Diagnostics are based in part on satellite sea ice climatology developed since the Scanning Multichannel Microwave Radiometer (SMMR) era in 1978.

3.5.2 Operational QA

AMSR-E Level-2A data arriving at GHCC are subject to operational QA prior to processing higher-level products. Operational QA varies by product, but it typically checks for the following criteria in a given file (Conway 2002):

- File is correctly named and sized
- File contains all expected elements
- File is in the expected format
- Required EOS fields of time, latitude, and longitude are present and populated
- Structural metadata is correct and complete
- The file is not a duplicate
- The HDF-EOS version number is provided in the global attributes
- The correct number of input files were available and processed

3.5.3 Science QA

AMSR-E Level-2A data arriving at GHCC are also subject to science QA prior to processing higher-level products. If less than 50 percent of a granule's data is good, the science QA flag is marked suspect when the granule is delivered to NSIDC. In the SIPS environment, the science QA includes checking the maximum and minimum variable values, and percent of missing data and out-of-bounds data per variable value. At the Science Computing Facility (SCF), also at GHCC, science QA involves reviewing the operational QA files, generating browse images, and performing the following additional automated QA procedures (Conway 2002):

- Historical data comparisons
- Detection of errors in geolocation
- Verification of calibration data
- Trends in calibration data
- Detection of large scatter among data points that should be consistent

Geolocation errors are corrected during Level-2A processing to prevent processing anomalies such as extended execution times and large percentages of out-of-bounds data in the products derived from Level-2A data.

The Team Lead SIPS (TLSIPS) developed tools for use at SIPS and SCF for inspecting the data granules. These tools generate a QA browse image in Portable Network Graphics (PNG) format and a QA summary report in text format for each data granule. Each browse file shows Level-2A and Level-2B data. These are forwarded from RSS to GHCC along with associated granule information, where they are converted to HDF raster images prior to delivery to NSIDC.

Refer to the AMSR-E Validation Data for information about data used to check the accuracy and precision of AMSR-E observations.

Refer to the AMSR-E Data Quality documentation for more information on quality assessment

3.6 Sensor or Instrument Description

Refer to the AMSR-E Instrument Description document.

4 REFERENCES AND RELATED PUBLICATIONS

Cavalieri, D. and J. Comiso. 2000. Algorithm Theoretical Basis Document for the AMSR-E Sea Ice Algorithm, Revised December 1. Landover, Maryland USA: Goddard Space Flight Center.

Cavalieri, D. J., K. M. St. Germain, and C.T . Swift. 1995. Reduction of Weather Effects in the Calculation of Sea Ice Concentration with the DMSP SSM/I. *Journal of Glaciology* 41(139): 455-464.

Cavalieri, D. J., P. Gloersen, and W. J. Campbell. 1984. Determination of Sea Ice Parameters with the NIMBUS-7 SMMR. *Journal of Geophysical Research* 89(D4): 5355-5369.

Colbeck, S. C. 1982. An Overview of Seasonal Snow Metamorphism. *Reviews of Geophysics Space Physics* 20:45-61.

Comiso, J., D. Cavalieri, and T. Markus. 2003. Sea Ice Concentration, Ice Temperature, and Snow Depth Using AMSR-E Data. *IEEE Transactions on Geoscience and Remote Sensing* 41(2): 243-252.

Comiso, J. and K. Steffen. 2001. Studies of Antarctic Sea Ice Concentrations from Satellite Data and Their Applications. *Journal of Geophysical Research* 106(C12): 31,361-31,385.

Comiso, J. C., D. J. Cavalieri, C. L. Parkinson, and P. Gloersen. 1997. Passive Microwave Algorithms for Sea Ice Concentration - A Comparison of Two Techniques. *Remote Sensing of the Environment* 60: 357-384.

Comiso, J. C. 1995. *SSM/I Ice Concentrations Using the Bootstrap Algorithm*. NASA RP 1380.

Conway, D. 2002. *Advanced Microwave Scanning Radiometer - EOS Quality Assurance Plan*. Huntsville, AL: Global Hydrology and Climate Center.

Eppler, D. T. and 14 others. 1992. Passive Microwave Signatures of Sea Ice. IN: *Microwave Remote Sensing of Ice*. *Geophysical Monograph Series* 68: 47-71. Washington, D. C.: American Geophysical Union.

Fraser R. S., N. E. Gaut, E. C. Reifenstein, and H. Sievering. 1975. Interaction Mechanisms Within the Atmosphere Including the Manual of Remote Sensing. *American Society of Photogrammetry* 181-233. Falls Church, VA.

Gloersen P. and D. J. Cavalieri. 1986. Reduction of Weather Effects in the Calculation of Sea Ice Concentration from Microwave Radiances. *Journal of Geophysical Research*91(C3): 3913-3919.

Kelly, R. E., A. T. C. Chang, L. Tsang, and J. L. Foster. 2003. A Prototype AMSR-E Global Snow Area and Snow Depth Algorithm. *IEEE Transactions Geoscience Remote Sensing* 41: 230-242.

Kummerow, C. 1993. On the Accuracy of the Eddington Approximation for Radiative Transfer in the Microwave Frequencies. *Journal of Geophysical Research* 98: 2757-2765.

Markus, Thorsten and Donald J. Cavalieri. 2008. [Supplement] AMSR-E Algorithm Theoretical Basis Document: Sea Ice Products. Greenbelt, Maryland USA: Goddard Space Flight Center. (PDF file, 2.10 MB)

Markus, T. and D. Cavalieri. 1998. Snow Depth Distribution over Sea Ice in the Southern Ocean from Satellite Passive Microwave Data. IN: *Antarctic Sea Ice: Physical Processes, Interactions, and Variability*. *Antarctic Research Series* 74: 19-39. Washington, DC: American Geophysical Union.

Markus, T., D. Cavalieri, and A. Ivanoff. 2011. Algorithm Theoretical Basis Document for the AMSR-E Sea Ice Algorithm, Revised December 2011. Landover, MD: Goddard Space Flight Center. (PDF file, 528 KB)

Markus, T. and D. Cavalieri. 2000. An Enhancement of the NASA Team Sea Ice Algorithm. *IEEE Transactions on Geoscience and Remote Sensing* 38: 1387-1398.

Matzler, C., R. O. Ramseier, and E. Svendsen. 1984. Polarization Effects in Sea-ice Signatures. *IEEE Journal of Oceanic Engineering* 9: 333-338.

Pearson, F. 1990. *Map projections: Theory and Applications*. Boca Raton, FL: CRC Press.

Snyder, J. P. 1987. *Map Projections - A Working Manual*. U.S. Geological Survey Professional Paper 1395. U.S. Government Printing Office. Washington, D.C.

Snyder, J. P. 1982. *Map Projections Used by the U.S. Geological Survey.* U.S. Geological Survey Bulletin 1532.

Worby, A. P., T. Markus, A. D. Steer, V. I. Lytle, and R. A. Massom. 2008. Evaluation of AMSR-E Snow Depth Product over East Antarctic Sea Ice Using In Situ Measurements and Aerial

Photography, *Journal of Geophysical Research* 113(C05): Art. #C05S94. doi:10.1029/2007JC004181.

For more information regarding related publications, see the Research Using AMSR-E Data Web page.

4.1 RELATED DATA COLLECTIONS

Sea Ice Products at NSIDC

This site offers a complete summary of sea ice data derived from passive microwave sensors and other sources, and is useful for users who want to compare characteristics of various sea ice products to understand their similarities and differences. This site also provides links to tools for passive microwave data and a list of other sea ice resources.

Sea Ice Trends and Climatologies from SMMR and SSM/I-SSMIS

This site provides a suite of value-added products to aid in investigations of the variability and trends of sea ice cover. These products provide users with information about sea ice extent, total ice covered area, ice persistence, monthly climatologies of sea ice concentrations, and ocean masks.

4.2 RELATED WEB SITES

Sea Ice Remote Sensing at NASA/Goddard Space Flight Center

5 CONTACTS AND ACKNOWLEDGMENTS

Investigator(s) Name and Title

Donald J. Cavalieri
Laboratory for Hydrospheric Processes
NASA Goddard Space Flight Center

Josefino Comiso
Laboratory for Hydrospheric Processes
NASA Goddard Space Flight Center

Thorsten Markus
Laboratory for Hydrospheric Processes
NASA Goddard Space Flight Center

6 DOCUMENT INFORMATION

6.1 Publication Date

May 2014

6.2 Date Last Updated

20 December 2021

APPENDIX A – LEVEL-3 12.5 KM SEA ICE DATA FIELDS

The following notations are used throughout this document:

Int8	8-bit (1-byte) signed integer
Int16	16-bit (2-byte) signed integer
NT2	Enhanced NASA Team algorithm
BBA	Bootstrap Basic Algorithm

The following tables give detailed descriptions for:

- North polar grids (608 pixels by 896 pixels)
- Northern Hemisphere masks (608 pixels by 896 pixels)
- South polar grids (632 pixels by 664 pixels)

North Polar Grids

Table A - 1. North Polar Grids

Field Name	**Data Type**	**Description**	**Scale Factor**
SI_12km_NH_18V_ASC	Int16	18.7 GHz horizontal daily average Brightness Temperatures (T_bs) (K) Valid range: approximately 50 to 300 K	Multiply data values by 0.1 to obtain units in K
SI_12km_NH_18V_DSC	Int16	18.7 GHz vertical daily average descending T_bs (K) Valid range: approximately 50 to 300 K	Multiply data values by 0.1 to obtain units in K
SI_12km_NH_18V_DAY	Int16	18.7 GHz vertical daily average T_bs (K) Valid range: approximately 50 to 300 K	Multiply data values by 0.1 to obtain units in K
SI_12km_NH_18H_ASC	Int16	18.7 GHz horizontal daily average ascending T_bs (K) Valid range: approximately 50 to 300 K	Multiply data values by 0.1 to obtain units in K
SI_12km_NH_18H_DSC	Int16	18.7 GHz horizontal daily average descending T_bs (K) Valid range: approximately 50 to 300 K	Multiply data values by 0.1 to obtain units in K

Field Name	Data Type	Description	Scale Factor
SI_12km_NH_18H_DAY	Int16	18.7 GHz horizontal daily average T_bs (K) Valid range: approximately 50 to 300 K	Multiply data values by 0.1 to obtain units in K
SI_12km_NH_23V_ASC	Int16	23.8 GHz vertical daily average ascending T_bs (K) Valid range: approximately 50 to 300 K	Multiply data values by 0.1 to obtain units in K
SI_12km_NH_23V_DSC	Int16	23.8 GHz vertical daily average descending T_bs (K) Valid range: approximately 50 to 300 K	Multiply data values by 0.1 to obtain units in K
SI_12km_NH_23V_DAY	Int16	23.8 GHz vertical daily average T_bs (K) Valid range: approximately 50 to 300 K	Multiply data values by 0.1 to obtain units in K
SI_12km_NH_23H_ASC	Int16	23.8 GHz horizontal daily average ascending T_bs (K) Valid range: approximately 50 to 300 K	Multiply data values by 0.1 to obtain units in K
SI_12km_NH_23H_DSC	Int16	23.8 GHz horizontal daily average descending T_bs (K) Valid range: approximately 50 to 300 K	Multiply data values by 0.1 to obtain units in K
SI_12km_NH_23H_DAY	Int16	23.8 GHz horizontal daily average T_bs (K) Valid range: approximately 50 to 300 K	Multiply data values by 0.1 to obtain units in K
SI_12km_NH_36V_ASC	Int16	36.5 GHz vertical daily average ascending T_bs (K) Valid range: approximately 50 to 300 K	Multiply data values by 0.1 to obtain units in K
SI_12km_NH_36V_DSC	Int16	36.5 GHz vertical daily average descending T_bs (K) Valid range: approximately 50 to 300 K	Multiply data values by 0.1 to obtain units in K
SI_12km_NH_36V_DAY	Int16	36.5 GHz vertical daily average T_bs (K) Valid range: approximately 50 to 300 K	Multiply data values by 0.1 to obtain units in K

Field Name	Data Type	Description	Scale Factor
SI_12km_NH_36H_ASC	Int16	36.5 GHz horizontal daily average ascending T_bs (K) Valid range: approximately 50 to 300 K	Multiply data values by 0.1 to obtain units in K
SI_12km_NH_36H_DSC	Int16	36.5 GHz horizontal daily average descending T_bs (K) Valid range: approximately 50 to 300 K	Multiply data values by 0.1 to obtain units in K
SI_12km_NH_36H_DAY	Int16	36.5 GHz horizontal daily average T_bs (K) Valid range: approximately 50 to 300 K	Multiply data values by 0.1 to obtain units in K
SI_12km_NH_89V_ASC	Int16	89.0 GHz vertical daily average ascending T_bs (K) Valid range: approximately 50 to 300 K	Multiply data values by 0.1 to obtain units in K
SI_12km_NH_89V_DSC	Int16	89.0 GHz vertical daily average descending T_bs (K) Valid range: approximately 50 to 300 K	Multiply data values by 0.1 to obtain units in K
SI_12km_NH_89V_DAY	Int16	89.0 GHz vertical daily average T_bs (K) Valid range: approximately 50 to 300 K	Multiply data values by 0.1 to obtain units in K
SI_12km_NH_89H_ASC	Int16	89.0 GHz horizontal daily average ascending T_bs (K) Valid range: approximately 50 to 300 K	Multiply data values by 0.1 to obtain units in K
SI_12km_NH_89H_DSC	Int16	89.0 GHz horizontal daily average descending T_bs (K) Valid range: approximately 50 to 300 K	Multiply data values by 0.1 to obtain units in K
SI_12km_NH_89H_DAY	Int16	89.0 GHz horizontal daily average T_bs (K) Valid range: approximately 50 to 300 K	Multiply data values by 0.1 to obtain units in K

<table>
<tr><th>Field Name</th><th>Data Type</th><th>Description</th><th>Scale Factor</th></tr>
<tr><td>SI_12km_NH_ICECON_ASC</td><td>Int16</td><td>Sea ice concentration daily ascending average<table><tr><th>Value</th><th>Description</th></tr><tr><td>0</td><td>Open Water</td></tr><tr><td>1 to 100</td><td>Percent Ice Concentration</td></tr><tr><td>120</td><td>Land Mask</td></tr></table></td><td>Not Applicable (N/A)</td></tr>
<tr><td>SI_12km_NH_ICECON_DSC</td><td>Int16</td><td>Sea ice concentration daily descending average<table><tr><th>Value</th><th>Description</th></tr><tr><td>0</td><td>Open Water</td></tr><tr><td>1 to 100</td><td>Percent Ice Concentration</td></tr><tr><td>120</td><td>Land Mask</td></tr></table></td><td>N/A</td></tr>
<tr><td>SI_12km_NH_ICECON_DAY</td><td>Int16</td><td>Sea ice concentration daily average<table><tr><th>Value</th><th>Description</th></tr><tr><td>0</td><td>Open Water</td></tr><tr><td>1 to 100</td><td>Percent Ice Concentration</td></tr><tr><td>120</td><td>Land Mask</td></tr></table></td><td>N/A</td></tr>
</table>

<table>
<tr><th>Field Name</th><th>Data Type</th><th>Description</th><th>Scale Factor</th></tr>
<tr><td>SI_12km_NH_ICEDIFF_ASC</td><td>Int16</td><td>Sea ice concentration daily ascending average using the difference between BBA and NT2 algorithms
<table>
<tr><th>Value</th><th>Description</th></tr>
<tr><td>0</td><td>Open Water</td></tr>
<tr><td>1 to 100 or -1 to -100</td><td>Percent difference between algorithms*</td></tr>
<tr><td>120</td><td>Land Mask</td></tr>
<tr><td>200 to 300</td><td>Missing NT2 value (200+BBA)**</td></tr>
<tr><td>-200 to -300</td><td>Missing BBA value (-200-NT2)**</td></tr>
<tr><td>-310</td><td>Out-of-range value in V12 data***</td></tr>
</table></td><td>N/A</td></tr>
<tr><td>SI_12km_NH_ICEDIFF_DSC</td><td>Int16</td><td>Sea ice concentration daily descending average using the difference between BBA and NT2 algorithms
<table>
<tr><th>Value</th><th>Description</th></tr>
<tr><td>0</td><td>Open Water</td></tr>
<tr><td>1 to 100 or -1 to -100</td><td>Percent difference between algorithms*</td></tr>
<tr><td>200 to 300</td><td>Missing NT2 value (200+BBA)**</td></tr>
<tr><td>-200 to -300</td><td>Missing BBA value (-200-NT2)**</td></tr>
<tr><td>-310</td><td>Out-of-range value in V12 data***</td></tr>
</table></td><td>N/A</td></tr>
</table>

<table>
<tr><th>Field Name</th><th>Data Type</th><th>Description</th><th>Scale Factor</th></tr>
<tr><td>SI_12km_NH_ICEDIFF_DAY</td><td>Int16</td><td>Sea ice concentration daily average using the difference between BBA and NT2 algorithms
<table><tr><th>Value</th><th>Description</th></tr><tr><td>0</td><td>Open Water</td></tr><tr><td>1 to 100 or -1 to -100</td><td>Percent difference between algorithms*</td></tr><tr><td>200 to 300</td><td>Missing NT2 value (200+BBA)**</td></tr><tr><td>-200 to -300</td><td>Missing BBA value (-200-NT2)**</td></tr><tr><td>-310</td><td>Out-of-range value in V12 data***</td></tr></table></td><td>N/A</td></tr>
<tr><td>SI_12km_NH_SNOWDEPTH_5DAY</td><td>Int16</td><td>5-day running average of snow depth (cm) based on current day and previous 4 days
<table><tr><th>Value</th><th>Description</th></tr><tr><td>110</td><td>Missing Data</td></tr><tr><td>120</td><td>Land Mask</td></tr><tr><td>130</td><td>Open Water</td></tr><tr><td>140</td><td>Multiyear Sea Ice</td></tr><tr><td>150</td><td>Variability in Snow Depth</td></tr><tr><td>160</td><td>Snow Melt</td></tr></table></td><td>N/A</td></tr>
</table>

Field Name	Data Type	Description	Scale Factor
* Positive values 1 to 100% represent the difference in concentration where NT2 is greater than BBA and negative values -1 to -100% represent the difference in concentration where BBA is greater than NT2. ** The difference values need input from both the NT2 and BBA sea ice concentration algorithms. These new values indicate when one of these is missing. If there is a valid BBA value and missing NT2, it takes on the value 200+BBA. Likewise, a valid NT2 and missing BBA takes on the value -200-NT2. A difference value of 200 means the BBA was open water and the NT2 was missing; a value of 225 means the BBA was 25% and the NT2 was missing. A value of 300 means BBA was 100 and NT2 was missing. The normal range of difference values is -100 to 100. *** An out-of-range value for the sea ice concentration difference field was introduced in Validated 12 (V12) AMSR-E 12.5 km sea ice data when data from the BBA were missing. The value was -310, whereas the standard value when BBA data are missing is -200 to -300. With V13 data, the data were updated to correct this issue. However, as past data will not be reprocessed, users should be mindful of this out-of-range value when working with data prior to 27 August 2010.			

Northern Hemisphere Masks

Beginning with Version 12 data, the Northern Hemisphere sea ice and snow melt masks used for the snow depth on sea ice parameter are stored within the 12.5 km product (AE_SI12). The following table describes the mask contents of the HDF files.

Table A - 2. Description of Sea Ice and Snow Melt Masks

Field Name	Data Type	Description	Dimensions	Scale Factor
date	Int16	The processing date (year/month/day) of the masks.	3	n/a
initialization year	Int16	The first year in which the mask was set, or reset, to begin processing.	1	n/a
multiyear mask	Int16	A multiyear sea ice mask.	608 x 896	n/a
variability 5day	Int16	A running 5-day snow melt mask corresponding to the running 5-day snow melt product.	608 x 896	n/a

South Polar Grids

Table A - 3. South Polar Grids

Field Name	Data Type	Description	Scale Factor
SI_12km_SH_18V_ASC	Int16	18.7 GHz horizontal daily average T_bs (K) Valid range: approximately 50 to 300 kelvin (K)	Multiply data values by 0.1 to obtain units in kelvin (K)
SI_12km_SH_18V_DSC	Int16	18.7 GHz vertical daily average descending T_bs (K) Valid range: approximately 50 to 300 K	Multiply data values by 0.1 to obtain units in K
SI_12km_SH_18V_DAY	Int16	18.7 GHz vertical daily average T_bs (K) Valid range: approximately 50 to 300 K	Multiply data values by 0.1 to obtain units in K
SI_12km_SH_18H_ASC	Int16	18.7 GHz horizontal daily average ascending T_bs (K) Valid range: approximately 50 to 300 K	Multiply data values by 0.1 to obtain units in K
SI_12km_SH_18H_DSC	Int16	18.7 GHz horizontal daily average descending T_bs (K) Valid range: approximately 50 to 300 K	Multiply data values by 0.1 to obtain units in K
SI_12km_SH_18H_DAY	Int16	18.7 GHz horizontal daily average T_bs (K) Valid range: approximately 50 to 300 K	Multiply data values by 0.1 to obtain units in K
SI_12km_SH_23V_ASC	Int16	23.8 GHz vertical daily average ascending T_bs (K) Valid range: approximately 50 to 300 K	Multiply data values by 0.1 to obtain units in K

Field Name	Data Type	Description	Scale Factor
SI_12km_SH_23V_DSC	Int16	23.8 GHz vertical daily average descending T_bs (K) Valid range: approximately 50 to 300 K	Multiply data values by 0.1 to obtain units in K
SI_12km_SH_23V_DAY	Int16	23.8 GHz vertical daily average T_bs (K) Valid range: approximately 50 to 300 K	Multiply data values by 0.1 to obtain units in K
SI_12km_SH_23H_ASC	Int16	23.8 GHz horizontal daily average ascending T_bs (K) Valid range: approximately 50 to 300 K	Multiply data values by 0.1 to obtain units in K
SI_12km_SH_23H_DSC	Int16	23.8 GHz horizontal daily average descending T_bs (K) Valid range: approximately 50 to 300 K	Multiply data values by 0.1 to obtain units in K
SI_12km_SH_23H_DAY	Int16	23.8 GHz horizontal daily average T_bs (K) Valid range: approximately 50 to 300 K	Multiply data values by 0.1 to obtain units in K
SI_12km_SH_36V_ASC	Int16	36.5 GHz vertical daily average ascending T_bs (K) Valid range: approximately 50 to 300 K	Multiply data values by 0.1 to obtain units in K
SI_12km_SH_36V_DSC	Int16	36.5 GHz vertical daily average descending T_bs (K) Valid range: approximately 50 to 300 K	Multiply data values by 0.1 to obtain units in K
SI_12km_SH_36V_DAY	Int16	36.5 GHz vertical daily average T_bs (K) Valid range: approximately 50 to 300 K	Multiply data values by 0.1 to obtain units in K

Field Name	Data Type	Description	Scale Factor
SI_12km_SH_36H_ASC	Int16	36.5 GHz horizontal daily average ascending T_bs (K) Valid range: approximately 50 to 300 K	Multiply data values by 0.1 to obtain units in K
SI_12km_SH_36H_DSC	Int16	36.5 GHz horizontal daily average descending T_bs (K) Valid range: approximately 50 to 300 K	Multiply data values by 0.1 to obtain units in K
SI_12km_SH_36H_DAY	Int16	36.5 GHz horizontal daily average T_bs (K) Valid range: approximately 50 to 300 K	Multiply data values by 0.1 to obtain units in K
SI_12km_SH_89V_ASC	Int16	89.0 GHz vertical daily average ascending T_bs (K) Valid range: approximately 50 to 300 K	Multiply data values by 0.1 to obtain units in K
SI_12km_SH_89V_DSC	Int16	89.0 GHz vertical daily average descending T_bs (K) Valid range: approximately 50 to 300 K	Multiply data values by 0.1 to obtain units in K
SI_12km_SH_89V_DAY	Int16	89.0 GHz vertical daily average T_bs (K) Valid range: approximately 50 to 300 K	Multiply data values by 0.1 to obtain units in K
SI_12km_SH_89H_ASC	Int16	89.0 GHz horizontal daily average ascending T_bs (K) Valid range: approximately 50 to 300 K	Multiply data values by 0.1 to obtain units in K
SI_12km_SH_89H_DSC	Int16	89.0 GHz horizontal daily average descending T_bs (K) Valid range: approximately 50 to 300 K	Multiply data values by 0.1 to obtain units in K

<table>
<tr><th>Field Name</th><th>Data Type</th><th>Description</th><th>Scale Factor</th></tr>
<tr><td>SI_12km_SH_89H_DAY</td><td>Int16</td><td>89.0 GHz horizontal daily average T_bs (K)
Valid range: approximately 50 to 300 K</td><td>Multiply data values by 0.1 to obtain units in K</td></tr>
<tr><td>SI_12km_SH_ICECON_ASC</td><td>Int16</td><td>Sea ice concentration daily ascending average
<table>
<tr><th>Value</th><th>Description</th></tr>
<tr><td>0</td><td>Open Water</td></tr>
<tr><td>1 to 100</td><td>Percent Ice Concentration</td></tr>
<tr><td>110</td><td>Not Calculated</td></tr>
<tr><td>120</td><td>Land Mask</td></tr>
</table></td><td>N/A</td></tr>
<tr><td>SI_12km_SH_ICECON_DSC</td><td>Int16</td><td>Sea ice concentration daily descending average
<table>
<tr><th>Value</th><th>Description</th></tr>
<tr><td>0</td><td>Open Water</td></tr>
<tr><td>1 to 100</td><td>Percent Ice Concentration</td></tr>
<tr><td>110</td><td>Not Calculated</td></tr>
<tr><td>120</td><td>Land Mask</td></tr>
</table></td><td>N/A</td></tr>
<tr><td>SI_12km_SH_ICECON_DAY</td><td>Int16</td><td>Sea ice concentration daily average
<table>
<tr><th>Value</th><th>Description</th></tr>
<tr><td>0</td><td>Open Water</td></tr>
<tr><td>1 to 100</td><td>Percent Ice Concentration</td></tr>
<tr><td>110</td><td>Not Calculated</td></tr>
<tr><td>120</td><td>Land Mask</td></tr>
</table></td><td>N/A</td></tr>
</table>

<table>
<tr><th>Field Name</th><th>Data Type</th><th>Description</th><th>Scale Factor</th></tr>
<tr><td>SI_12km_SH_ICEDIFF_ASC</td><td>Int16</td><td>Sea ice concentration daily ascending average using the difference between BBA and NT2 algorithms
<table>
<tr><th>Value</th><th>Description</th></tr>
<tr><td>0</td><td>Open Water</td></tr>
<tr><td>1 to 100 or -1 to -100</td><td>Percent difference between algorithms*</td></tr>
<tr><td>110</td><td>Not Calculated</td></tr>
<tr><td>120</td><td>Land Mask</td></tr>
<tr><td>200 to 300</td><td>Missing NT2 value (200+BBA)**</td></tr>
<tr><td>-200 to -300</td><td>Missing BBA value (-200-NT2)**</td></tr>
<tr><td>-310</td><td>Out-of-range value in V12 data***</td></tr>
</table></td><td>N/A</td></tr>
</table>

<table>
<tr><th>Field Name</th><th>Data Type</th><th>Description</th><th>Scale Factor</th></tr>
<tr><td>SI_12km_SH_ICEDIFF_DSC</td><td>Int16</td><td>Sea ice concentration daily descending average using the difference between BBA and NT2 algorithms
<table>
<tr><th>Value</th><th>Description</th></tr>
<tr><td>0</td><td>Open Water</td></tr>
<tr><td>1 to 100 or -1 to -100</td><td>Percent difference between algorithms*</td></tr>
<tr><td>110</td><td>Not Calculated</td></tr>
<tr><td>120</td><td>Land Mask</td></tr>
<tr><td>200 to 300</td><td>Missing NT2 value (200+BBA)**</td></tr>
<tr><td>-200 to -300</td><td>Missing BBA value (-200-NT2)**</td></tr>
<tr><td>-310</td><td>Out-of-range value in V12 data***</td></tr>
</table></td><td>N/A</td></tr>
</table>

<table>
<tr><th>Field Name</th><th>Data Type</th><th>Description</th><th>Scale Factor</th></tr>
<tr><td>SI_12km_SH_ICEDIFF_DAY</td><td>Int16</td><td>Sea ice concentration daily average using the difference between BBA and NT2 algorithms
<table>
<tr><th>Value</th><th>Description</th></tr>
<tr><td>0</td><td>Open Water</td></tr>
<tr><td>1 to 100 or -1 to -100</td><td>Percent difference between algorithms*</td></tr>
<tr><td>110</td><td>Not Calculated</td></tr>
<tr><td>120</td><td>Land Mask</td></tr>
<tr><td>200 to 300</td><td>Missing NT2 value (200+BBA)**</td></tr>
<tr><td>-200 to -300</td><td>Missing BBA value (-200-NT2)**</td></tr>
<tr><td>-310</td><td>Out-of-range value in V12 data***</td></tr>
</table></td><td>N/A</td></tr>
<tr><td>SI_12km_SH_SNOWDEPTH_5DAY</td><td>Int16</td><td>5-day running average of snow depth (cm) based on current day and previous 4 days
<table>
<tr><th>Value</th><th>Description</th></tr>
<tr><td>110</td><td>Not Calculated</td></tr>
<tr><td>120</td><td>Land Mask</td></tr>
<tr><td>130</td><td>Open Water</td></tr>
<tr><td>140</td><td>Multiyear Sea Ice</td></tr>
<tr><td>150</td><td>Variability in Snow Depth</td></tr>
<tr><td>160</td><td>Snow Melt</td></tr>
</table></td><td>N/A</td></tr>
</table>

Field Name	Data Type	Description	Scale Factor
* Positive values 1 to 100% represent the difference in concentration where NT2 is greater than BBA and negative values -1 to -100% represent the difference in concentration where BBA is greater than NT2. ** The difference values need input from both the NT2 and BBA sea ice concentration algorithms. These new values indicate when one of these is missing. If there is a valid BBA value and missing NT2, it takes on the value 200+BBA. Likewise, a valid NT2 and missing BBA takes on the value -200-NT2. A difference value of 200 means the BBA was open water and the NT2 was missing; a value of 225 means the BBA was 25% and the NT2 was missing. A value of 300 means BBA was 100 and NT2 was missing. The normal range of difference values is -100 to 100. *** An out-of-range value for the sea ice concentration difference field was introduced in Validated 12 (V12) AMSR-E 12.5 km sea ice data when data from the BBA were missing. The value was -310, whereas the standard value when BBA data are missing is -200 to -300. With V13 data, the data were updated to correct this issue. However, as past data will not be reprocessed, users should be mindful of this out-of-range value when working with data prior to 27 August 2010.			